UC Riverside

UC Riverside Previously Published Works

Title

H7N9 and other pathogenic avian influenza viruses elicit a three-pronged transcriptomic signature that is reminiscent of 1918 influenza virus and is associated with lethal outcome in mice.

Permalink

https://escholarship.org/uc/item/8j3744pf

Journal

Journal of virology, 88(18)

ISSN

0022-538X

Authors

Morrison, Juliet
Josset, Laurence
Tchitchek, Nicolas
et al.

Publication Date

2014-09-01

DOI

10.1128/jvi.00570-14

Peer reviewed

eScholarship.org Powered by the California Digital Library
University of California

JVI Journals.ASM.org

H7N9 and Other Pathogenic Avian Influenza Viruses Elicit a Three-Pronged Transcriptomic Signature That Is Reminiscent of 1918 Influenza Virus and Is Associated with Lethal Outcome in Mice

Juliet Morrison,[a] Laurence Josset,[a] Nicolas Tchitchek,[a] Jean Chang,[a] Jessica A. Belser,[b] David E. Swayne,[c] Mary J. Pantin-Jackwood,[c] Terrence M. Tumpey,[b] Michael G. Katze[a]

Department of Microbiology, School of Medicine, University of Washington, Seattle, Washington, USA[a]; Influenza Division, National Center for Immunization and Respiratory Diseases, Centers for Disease Control and Prevention, Atlanta, Georgia, USA[b]; Southeast Poultry Research Laboratory, Agricultural Research Service, U.S. Department of Agriculture, Athens, Georgia, USA[c]

ABSTRACT

Modulating the host response is a promising approach to treating influenza, caused by a virus whose pathogenesis is determined in part by the reaction it elicits within the host. Though the pathogenicity of emerging H7N9 influenza virus in several animal models has been reported, these studies have not included a detailed characterization of the host response following infection. Therefore, we characterized the transcriptomic response of BALB/c mice infected with H7N9 (A/Anhui/01/2013) virus and compared it to the responses induced by H5N1 (A/Vietnam/1203/2004), H7N7 (A/Netherlands/219/2003), and pandemic 2009 H1N1 (A/Mexico/4482/2009) influenza viruses. We found that responses to the H7 subtype viruses were intermediate to those elicited by H5N1 and pdm09H1N1 early in infection but that they evolved to resemble the H5N1 response as infection progressed. H5N1, H7N7, and H7N9 viruses were pathogenic in mice, and this pathogenicity correlated with increased transcription of cytokine response genes and decreased transcription of lipid metabolism and coagulation signaling genes. This three-pronged transcriptomic signature was observed in mice infected with pathogenic H1N1 strains such as the 1918 virus, indicating that it may be predictive of pathogenicity across multiple influenza virus strains. Finally, we used host transcriptomic profiling to computationally predict drugs that reverse the host response to H7N9 infection, and we identified six FDA-approved drugs that could potentially be repurposed to treat H7N9 and other pathogenic influenza viruses.

IMPORTANCE

Emerging avian influenza viruses are of global concern because the human population is immunologically naive to them. Current influenza drugs target viral molecules, but the high mutation rate of influenza viruses eventually leads to the development of antiviral resistance. As the host evolves far more slowly than the virus, and influenza pathogenesis is determined in part by the host response, targeting the host response is a promising approach to treating influenza. Here we characterize the host transcriptomic response to emerging H7N9 influenza virus and compare it with the responses to H7N7, H5N1, and pdm09H1N1. All three avian viruses were pathogenic in mice and elicited a transcriptomic signature that also occurs in response to the legendary 1918 influenza virus. Our work identifies host responses that could be targeted to treat severe H7N9 influenza and identifies six FDA-approved drugs that could potentially be repurposed as H7N9 influenza therapeutics.

Avian influenza virus strains with the potential to acquire human-to-human transmission are of global concern. Since the first human case of highly pathogenic avian H5N1 influenza virus was documented in China in 1997, there have been over 600 cases (1). More than half were fatal, primarily as a result of virus transmission from domestic poultry to humans (1). Despite the severity of disease and high fatality rate, H5N1 cases have remained sporadic, likely due to poor human-to-human transmissibility of the virus (2, 3). H7 subtype viruses have caused numerous small outbreaks over the past few decades (4–6). Notably, an H7N7 outbreak occurred in 2003 in the Netherlands, causing 89 confirmed human infections and 1 death (5). In early 2013, H7N9 avian influenza virus emerged in China, causing over 400 cases of influenza and more than 100 deaths between February 2013 and February 2014 (7–11). Phylogenetic analysis demonstrated that the novel H7N9 virus is a triple reassortant comprising a hemagglutinin (HA) from an avian H7N3 virus, the neuraminidase (NA) of an avian H7N9 virus, and all six internal genes from an avian H9N2 virus (10).

Though reports describe H7N9 viruses as less pathogenic than H5N1 in humans and animal models, H7N9 viruses are more transmissible than H5N1 in the direct-contact ferret model (12–16). Furthermore, some H7N9 viruses are able to bind human (α2,6-sialic acid) and avian (α2,3-sialic acid) receptors, though their avidity for human receptors is low (13–15, 17–19). In addition, H7N9 elicits a transcriptomic response intermediary to that induced by H5N1 or a human seasonal virus in cultured human airway epithelial cells, suggesting adaptation of H7N9 to its human host (20). These observations, combined with the fact that

Received 24 February 2014 **Accepted** 22 June 2014
Published ahead of print 2 July 2014
Editor: T. S. Dermody
Address correspondence to Michael G. Katze, honey@u.washington.edu.
Copyright © 2014, American Society for Microbiology. All Rights Reserved.
doi:10.1128/JVI.00570-14

Downloaded from http://jvi.asm.org/ on May 4, 2017 by COLUMBIA UNIVERSITY

H7N9 is more pathogenic than seasonal influenza virus strains, have sparked global concern (1, 11).

Influenza virus pathogenicity is due in part to the cytopathic effects of viral replication and the tissue damage that arises from an overly robust immune response. 1918 H1N1, which caused the deadliest recorded influenza pandemic, is thought to have caused severe disease and death in part because it elicited a highly aberrant immune response in the host (21). H5N1, which is even more pathogenic than 1918 H1N1 in mice, elicits a stronger and more accelerated response that is distinguishable from the response to 1918 H1N1 because of an earlier induction of inflammatory cytokine and lipoxin signaling genes (22).

There have been multiple reports characterizing the pathogenicity of H7N9 in different animal models, but these studies have not included detailed transcriptomic characterization of the host response. Additionally, no such characterization has been done for H7N7 (A/Netherlands/219/2003), an H7 subtype virus that was isolated from a fatal case of influenza and has a lethality similar to that of H7N9 in mammals (23–26). We previously conducted transcriptional profiling of the host response to H7N9 and H7N7 in cultured airway epithelial cells, which serve as a model of lung epithelial cells, and used it to predict new anti-H7N9 molecules (20). However, since multiple cell types participate in the host response to influenza, considering the contribution of different cell types to host response and disease progression delivers additional targets for host-directed interventions. We characterized, for the first time, the lung transcriptomic response of BALB/c mice infected with H7N9 (A/Anhui/1/2013) and compared it to the responses elicited by H5N1 (A/Vietnam/1203/2004), H7N7 (A/Netherlands/219/2003), and pdm09H1N1 (A/Mexico/4482/2009).

We found that lung responses to Anhui1 and NL219 were overall most similar to each other and intermediate to those elicited by VN1203 and Mex4482. Though H7N7 induced a more robust interferon and cytokine response than did H7N9 on day 1, the responses of the three avian viruses were remarkably similar later on in infection. All three avian viruses were pathogenic in mice, and increased pathogenicity correlated with increased induction of cytokine response genes and decreased transcription of lipid metabolism and coagulation signaling genes. This three-pronged transcriptomic signature may be predictive of influenza pathogenicity in mice across different viral strains, since it also occurs in response to 1918 H1N1 and mouse-adapted pdm09H1N1 (A/California/04/2009) virus (27). Finally, we used host transcriptional profiles to computationally identify drugs that may have therapeutic effects against H7N9 infection, identifying six FDA-approved drugs that could potentially be repurposed as H7N9 influenza therapeutics.

MATERIALS AND METHODS

Viruses. Three avian-origin influenza viruses isolated from fatal human cases, A/Anhui/01/2013 (H7N9), A/Netherlands/219/2003 (H7N7), and A/Vietnam/1203/2004 (H5N1), and a pandemic 2009 H1N1 (pdm09H1N1) human virus, A/Mexico/4482/2007, were used in this study. Virus stocks were grown in the allantoic cavities of 10-day-old embryonated hen's eggs for 24 to 28 h (high-pathogenicity avian influenza virus [HPAI]) or 48 h (low-pathogenicity avian influenza virus [LPAI]) at 37°C for avian-origin influenza viruses or for 48 h at 34°C for the pdm09H1N1 virus. Allantoic fluid from multiple eggs was pooled, clarified by centrifugation, aliquoted, and stored at −70°C. Virus titers were determined by plaque assay as previously described (28). All research with avian viruses was conducted under biosafety level 3 containment, including enhancements required by the U.S. Department of Agriculture and the Select Agent Program (http://www.cdc.gov/od/ohs/biosfty/bmbl5/bmbl5toc.htm).

Mouse infections. Six- to 8-week-old BALB/c mice were purchased from Charles River Laboratories (Wilmington, MA). All experiments were performed under biosafety level 3 enhanced containment. Mice were anesthetized with 2,2,2-tribromoethanol in *tert*-amyl alcohol (Avertin; Sigma-Aldrich, St. Louis, MO) and then inoculated intranasally with 50 μl of phosphate-buffered saline (mock infection) or with 10^5 PFU of virus in a 50-μl volume. Six animals in each virus-inoculated group were monitored for morbidity and mortality as measured by weight loss and survival over a period of 14 days. For transcriptomic profiling, mouse lungs were harvested from 5 virus-infected and 3 mock-infected mice on days 1, 3, and 5 postinfection. For viral titer measurements, lungs were collected from 4 virus-infected mice at each time point on days 1, 3, and 5 postinoculation. Animal research was conducted under the guidance of the CDC's Institutional Animal Care and Use Committee in an animal facility accredited by the Association for Assessment and Accreditation of Laboratory Animal Care International.

Histopathology. Lung sections were fixed by submersion in 10% neutral buffered formalin, routinely processed, and embedded in paraffin. Sections were made at 5 μm and were stained with hematoxylin and eosin (H&E).

RNA isolation and microarray processing. RNA extraction from virus- and mock-infected BALB/c mice was performed in quadruplicate as previously described (27). Probe labeling and microarray slide hybridization for each biological replicate were performed using the Whole Mouse Genome Microarray 4x44K kit (Agilent Technologies) according to the manufacturer's instructions. Slides were scanned on an Agilent DNA microarray scanner (model G2505B) using the extended dynamic range (XDR) setting, and raw images were analyzed using Agilent Feature Extraction software (version 9.5.3.1). Extracted raw data were background corrected using the "norm-exp" method with an offset of 1 and quantile normalized using the limma package (29) in the R environment. Replicated probes were mean summarized. All probes were required to pass the Agilent quality control (QC) flag ("gIsFound," "gIsWellAboveBG," "gIsSaturated," "gIsFeatNonUnifOL," and "gIsFeatPopnOL") for all replicates of at least one time point (29,382 probes passed QC filtering). For each sample, a log2 fold change (log2FC) value was calculated as the difference between log2-normalized data for this sample and the average of log2-normalized data for time-matched mock-infected samples. Microarray annotation was retrieved using the R package mgug4122a.db.

Identification of differentially expressed (DE) genes. Differential expression was determined by comparing influenza virus-infected replicates to time-matched mock-infected samples based on a linear model fit for each probe using the R package limma (29). Criteria for differential expression were an absolute log2FC of 1 and a q value of <0.05, calculated using a moderated *t* test with subsequent Benjamini-Hochberg correction.

Transcriptomic-distance analysis. To visualize the differences among biological samples in a 2-dimensional space, we used multidimensional scaling (MDS) representation (30). Euclidian distances between transcriptomics profiles were calculated based on normalized data, and nonmetric MDS was performed with the MASS package in R Bioconductor (31) to map the distances into the 2-dimensional space with minimal loss of information (evaluated by Kruskal's stress). Biological replicates from a same condition were linked in convex hulls (i.e., polygons) using the function "chull" in R.

Functional enrichment and drug prediction. Functional analysis of statistically significant gene expression changes was performed using Ingenuity Pathway Analysis (IPA; Ingenuity Systems). For all gene set enrichment analyses, a right-tailed Fisher exact test was used to calculate the probability that enrichment of each biological function was due to chance alone. All enrichment scores were calculated in IPA using the probes that passed our QC filter as the background data set. IPA upstream regulator

Downloaded from http://jvi.asm.org/ on May 4, 2017 by COLUMBIA UNIVERSITY

analysis, which is based on prior knowledge of expected effects between regulators and their known target genes according to the IPA database, was used to predict regulators and infer their activation state. The Z score determines whether gene expression changes for known targets of each regulator are consistent with what is expected from the literature (Z score > 2) or if the changes are anticorrelated with the literature (Z score < -2). To predict potential antivirals, the IPA database was queried with lists of DE genes from days 1 and 3 postinoculation in H7N9-infected mice, and we selected all the molecules annotated "drugs and chemicals" with Z scores less than -2. Z scores for the other three viruses were also noted (data not shown).

Computational measurement of immune cell subsets. To predict the immune cell composition of the virus-infected lungs, we defined immune cell genes as those genes that were expressed 20-fold more in an immune cell type than in lung tissue based on microarray data from GeneAtlas v3. Interferon-stimulated genes were removed from these lists so as to only consider genes specific to immune cells. The enrichment score (ES) for DE genes in each of these immune subsets was calculated as the $-\log10(P$ value) determined by the Fisher exact test. High ES in a specific immune cell population, e.g., granulocyte, indicates that a large number of genes upregulated after infection are highly expressed in granulocytes compared to lungs and therefore may result from granulocyte infiltration of the lungs.

Microarray data accession number. Raw microarray data were deposited in NCBI's Gene Expression Omnibus under accession number GSE54048.

RESULTS

H7N9, H7N7, and H5N1 are more pathogenic than pdm09H1N1 despite having similar replication levels. Previous reports have described human isolates of H7N9, H7N7, and H5N1 as highly pathogenic in BALB/c mice (13, 14, 19, 23, 25, 26, 32–36). To corroborate those findings and directly compare the replication levels and pathogenicities of the viruses, BALB/c mice were inoculated with 10^5 PFU of H7N9 (A/Anhui/01/2013), H7N7 (A/Netherlands/219/2003), H5N1 (A/Vietnam/1203/2004), or pdm09H1N1 (A/Mexico/4482/2007) virus (Fig. 1). The three avian viruses induced continuous weight loss in the mice, while Mex4482 did not (Fig. 1A). Mice infected with VN1203 died by 7 days postinoculation, while Anhui1- and NL219-infected mice died by 8 days postinoculation (Fig. 1B). None of the Mex4482-inoculated mice perished. Thus, Mex4482 was not pathogenic at a dose of 10^5 PFU in mice, whereas the avian viruses were highly pathogenic. Notably, the weight loss and survival differences were not attributable to differences in viral replication, given that all four viruses replicated to similar levels in the lungs, with titers peaking at $\sim10^6$ PFU/ml on day 3 (Fig. 1C).

The global transcriptional responses to H7N9 and H7N7 are intermediate to the responses induced by H5N1 and pdm09H1N1. To visualize the differences among the transcriptional responses, we utilized multidimensional scaling (MDS) (Fig. 2A). MDS aims to represent high-dimensional transcriptional profiles in a two-dimensional space for visualization purposes. The distance between two points on an MDS representation is proportional to their transcriptional difference, with small distances indicating similarity and large distances indicating dissimilarity. The transcriptional responses formed distinct clusters with respect to time postinfection and virus strain, indicating that there was consensus among biological replicates (Fig. 2A).

By focusing on the distance between each experimental condition (Fig. 2A), we were able to discern that (i) the host responses to VN1203 and Mex4482 were the most different from each other;

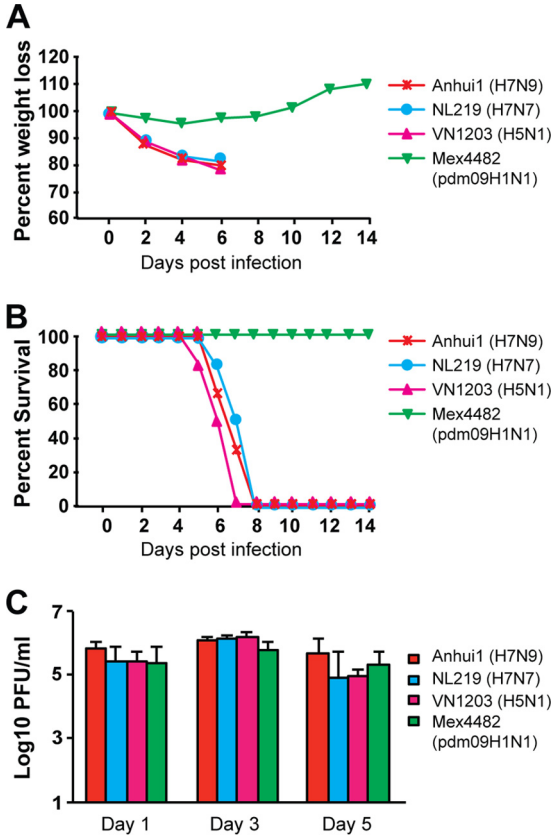

FIG 1 H7N9, H7N7, H5N1, and pdm09H1N1 display different pathogenicities but replicate to similar levels in BALB/c mice. BALB/c mice were infected with 10^5 PFU of H7N9 (A/Anhui/1/2013), H7N7 (A/Netherlands/219/2003), H5N1 (A/Vietnam/1203/2004), or pdm09H1N1 (A/Mexico/4482/2009). Following challenge, mice were monitored daily for weight loss (A) and survival (B) for 14 days. (C) BALB/c lungs were harvested at days 1, 3, and 5 postinfection, and their viral titers were quantitated using plaque assay (limit of detection = 10 PFU).

(ii) the responses to H7 subtype viruses were intermediate to the responses induced by VN1203 and Mex4482, with the Anhui1 response more similar to the Mex4482 response and the NL219 response more similar to the VN1203 response, especially at day 1 postinfection; and (iii) the host responses to the three avian viruses were remarkably similar to each other on day 3 postinfection but very different from the response to Mex4482 (Fig. 2A).

H7N9, H7N7, and H5N1 induce a more robust host response than does pdm09H1N1. To elucidate if the pathogenicity of each virus was related to the timing and magnitude of the host response, we compared the differentially expressed (DE) genes induced by infection with each virus versus mock infection at each time point (Fig. 2B). Each virus induced the differential expression of similar numbers of genes at day 1 (Fig. 2B). By day 3, there were more than 2,000 DE genes in Anhui1-, Mex4482-, and NL219-infected lungs and over 3,000 DE genes in VN1203-infected lungs (Fig. 2B). At day 5, the avian viruses induced differential expression of more than 3,000 genes, more than twice the number observed in Mex4482-infected animals. These data suggest that the host responses to the avian viruses were more robust and prolonged than the response to Mex4482, and they are consistent with the MDS plot (Fig. 2A), which shows that the Euclid-

Downloaded from http://jvi.asm.org/ on May 4, 2017 by COLUMBIA UNIVERSITY

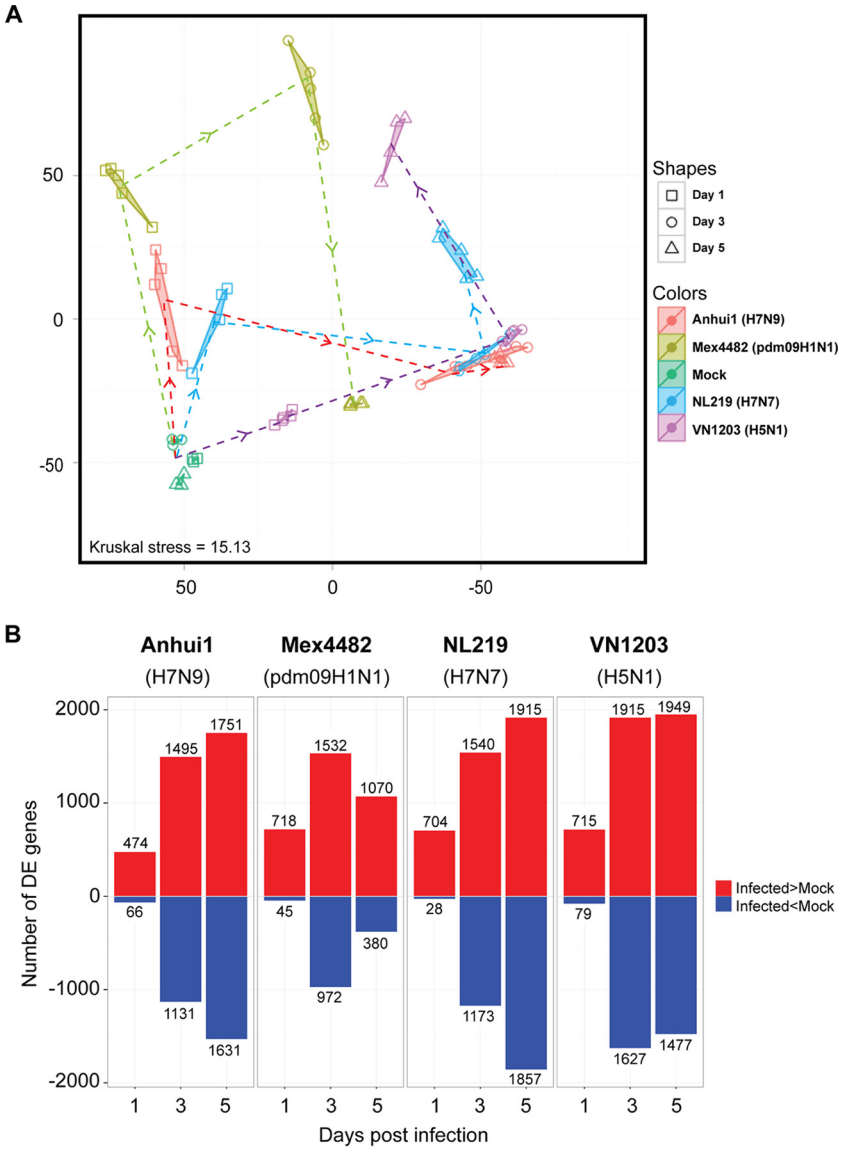

FIG 2 The global transcriptional responses to H7N9 and H7N7 are intermediate to the global transcriptional responses to H5N1 and pdm09H1N1. (A) Nonparametric multidimensional scaling (MDS) was used to show the Euclidean distance between experimental outcomes. Each mRNA sample is represented as a single point colored by viral condition and with different shapes according to time postinfection. Dotted lines and arrows represent the progression of the host response over time. The Kruskal stress criterion quantifies the quality of the representation as a fraction of the information lost during the dimensionality reduction procedure. (B) Number of upregulated and downregulated differentially expressed (DE) genes after infection with influenza virus. The DE genes in each infected sample were compared to time-matched mock-infected samples. Criteria used for differential expression analysis were a q value of <0.05 as determined by limma's empirical Bayes-moderated *t* test and $|\log_2 FC|>1$.

ean distance between Mex4482 and mock infections increased at day 3 and then decreased on day 5, demonstrating that the response to Mex4482 was returning to baseline. Thus, the host response to Mex4482 appeared to be resolving on day 5, while those to the avian viruses were progressing.

The H7N9 and H7N7 transcriptional programs share features with the pdm09H1N1 program on day 1 postinfection. As mentioned previously, H7N9 has features that are associated with human influenza viruses (15, 17). We therefore wanted to assess the similarity of the host responses to Ahnui1 and NL219 to that of a human virus, Mex4482, and to a prototypic pathogenic avian virus, VN1203. To do so, we used the manually curated data within Ingenuity Pathway Analysis (IPA) to identify biological pathways induced by each of the four viruses. On day 1, none of the top five pathways that were perturbed by VN1203 (as indicated by enrichment scores) were perturbed by Mex4482, again suggesting that these two viruses elicited vastly different host responses (Fig. 3A). However, there was overlap of the pathways affected by Anhui1, NL219, and Mex4482, indicating that these viruses were perturbing certain aspects of the host response in similar ways. For example, genes associated with the coagulation system and liver X receptor/retinoid X receptor (LXR/RXR) activation were highly differentially expressed in Anhui1-, NL219-, and Mex4482-infected lungs. Genes encoding thrombin (F2),

Downloaded from http://jvi.asm.org/ on May 4, 2017 by COLUMBIA UNIVERSITY

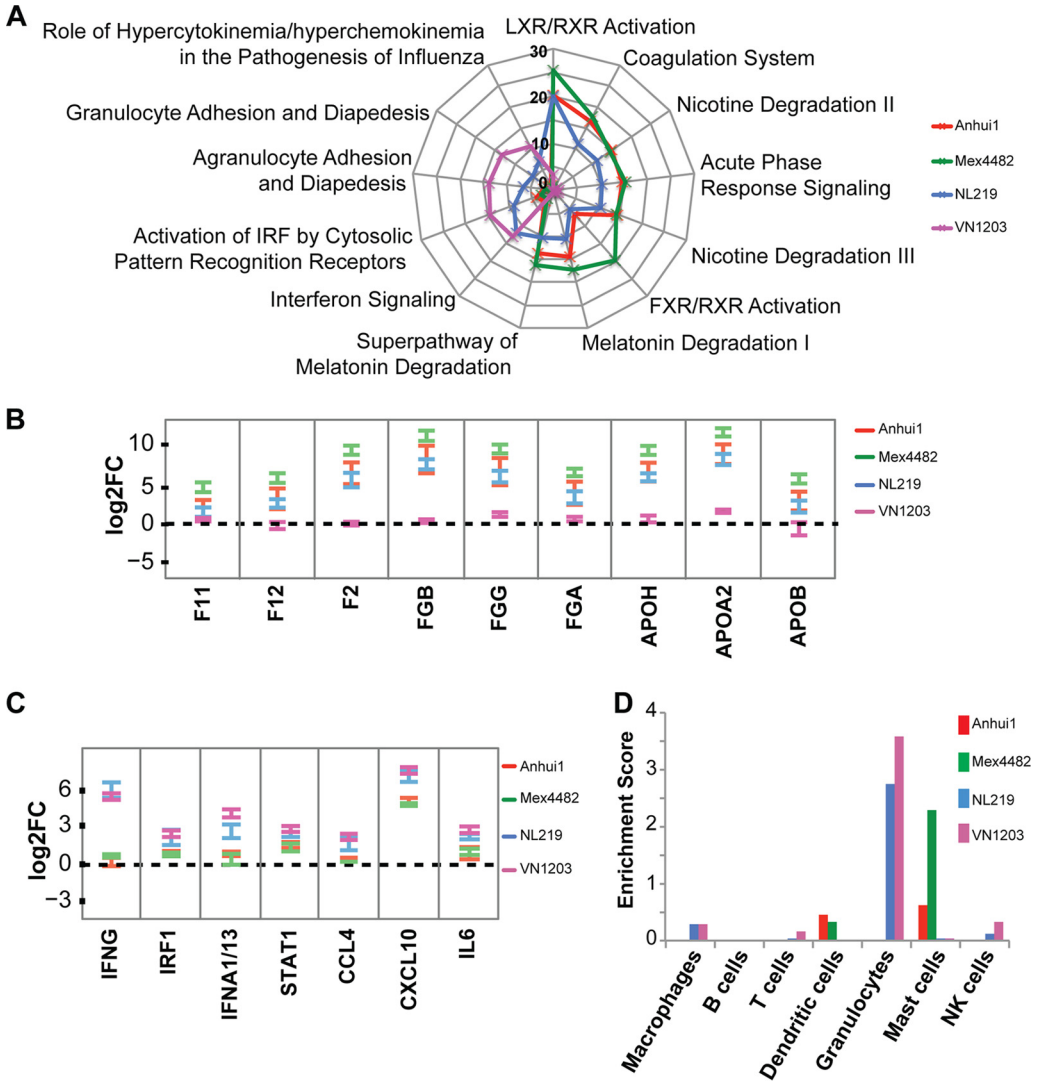

FIG 3 The H7N9 and H7N7 transcriptional programs differ on day 1 postinfection. The DE genes from Fig. 2 were analyzed with Ingenuity Pathway Analysis (IPA) to produce lists of host pathways that were most perturbed by infection with each virus at day 1. (A)The top 5 enriched pathways are represented as radial plots at day 1. The distance from the center in each radial plot represents the enrichment score (ES), which is defined as −log10(*P* value) using a right-tailed Fisher exact test. (B) Expression levels of select coagulation and lipid metabolism genes on day 1. (C) Expression levels of select interferon signaling and cytokine genes on day 1. (D) Computational measurement of immune cell subsets. Genes that were specifically upregulated in immune cells compared to lung tissue were defined as genes expressed 20-fold more in each immune cell type than in lungs on day 1 based on microarray analysis from GeneAtlas v3. Enrichment scores for DE genes in each of these immune subsets was calculated as −log10(*P* value) determined by Fisher exact test.

coagulation factor XII (F12), coagulation factor XI B (F11b), fibrinogen chain alpha (FGA), fibrinogen chain beta (FGB), and fibrinogen chain gamma (FGG) were expressed at low levels in VN1203-infected mice but were induced in mice infected with Anhui1, NL219, or Mex4482 (Fig. 3B). LXR/RXR pathway genes that were differentially expressed encoded molecules such as apolipoprotein H (APOH), apolipoprotein A2 (APOA2), and apolipoprotein B (APOB), which are components of lipid metabolism pathways.

There were, however, subtle differences between the responses to Anhui1 and NL219 on day 1. The H7 subtype viruses differed from each other with respect to their effects on interferon signaling (Fig. 3A and C). NL219, but not Anhui1, infection resulted in the expression of gamma interferon (IFN-γ), alpha interferon (IFNA1/IFNA13), signaling transducer and activator of transcription 1 (STAT1), and interferon regulatory factor 1 (IRF1) (Fig. 3B). Notably, the expression of these genes also contributed to the similarity of the NL219 response to the VN1203 response and of the Anhui1 response to the Mex4482 response. VN1203-infected mice showed upregulated transcription of these genes, while Mex4482-infected mice did not. The induction of cytokine genes such as those for interleukin 6 (IL-6), CXCL10, and CCL4 also divided NL219 and Anhui1 on day 1, with NL219 and VN1203 inducing transcription of these genes more highly than Anhui1 and Mex4482 did (Fig. 3C).

One consequence of the cytokine response is the recruitment of immune cells to the site of infection or damage. We took an integrative statistical approach to infer and categorize the different immune cell types that were present in the lungs on day 1. First, the GeneAtlas v3 database was used to identify genes associated

Downloaded from http://jvi.asm.org/ on May 4, 2017 by COLUMBIA UNIVERSITY

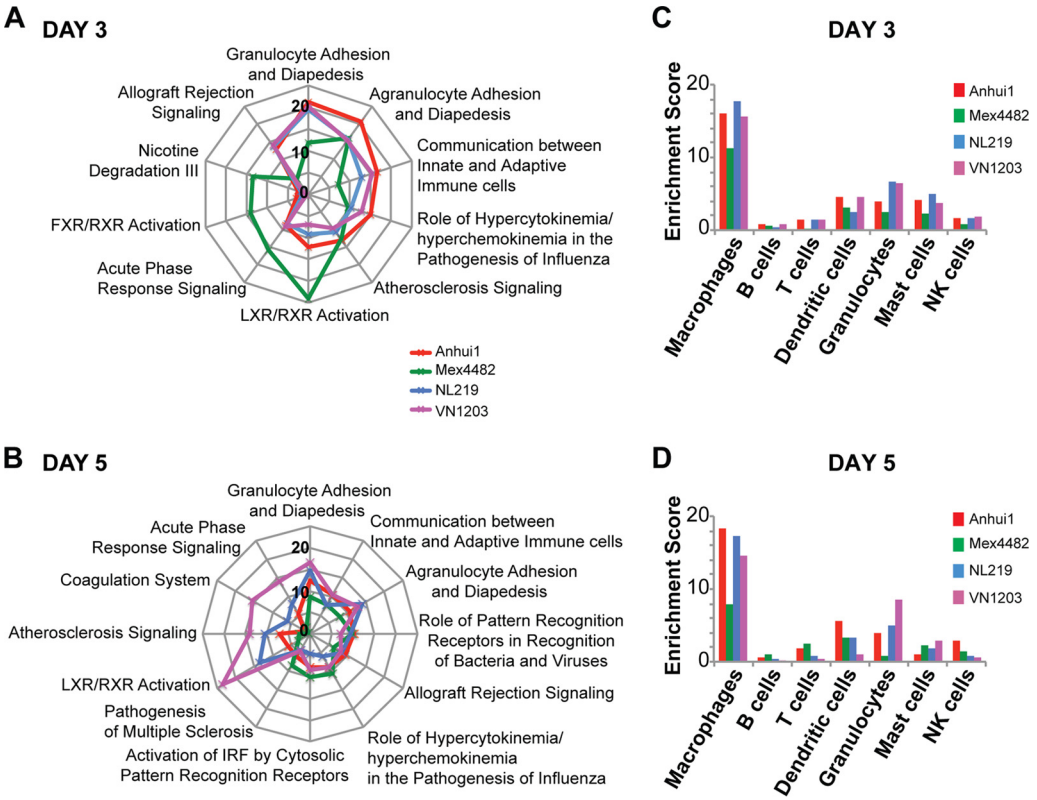

FIG 4 The host responses to the avian viruses are similar at later times postinfection. The DE genes from Fig. 2 were analyzed with Ingenuity Pathway Analysis (IPA) to produce lists of host pathways that were most perturbed by infection with each virus at day 3 (A) and day 5 (B). The top 5 enriched pathways are represented as radial plots at each time point. The distance from the center in each radial plots represents the enrichment score (ES) defined as −log10(*P* value) using a right-tailed Fisher exact test. (C and D) Computational measurement of immune cell subsets. Genes specifically upregulated in immune cells compared to lung tissue on day 3 (C) and day 5 (D) were defined as genes expressed 20-fold more in each immune cell type than in lungs based on microarray analysis from GeneAtlas v3. Enrichment scores for DE genes in each of these immune subsets was calculated as −log10(*P* value) determined by Fisher exact test.

with specific immune cell types. If these genes were induced 20-fold or more in a sample, we then inferred that immune cell types that express them were present in the lungs. A high enrichment score in a specific immune cell population, e.g., granulocytes, indicates that a large number of genes upregulated after infection are highly expressed in granulocytes compared to lung cells and therefore may result from granulocyte infiltration of the lungs. Mast cells appeared to be recruited to Mex4482-infected lungs (and, to a lesser extent, to Anhui1-infected lungs) but not to VN1203- and NL219-infected cells on day 1. Infection with VN1203 or NL219 but not Anhui1 or Mex4482 also appeared to trigger granulocyte infiltration (Fig. 3C), which has been implicated in influenza pathogenicity (37, 38). However, the three avian viruses had similar pathogenicities in mice, indicating that these day 1 differences were not determining pathogenicity in these experiments.

The later host responses to H7N9, H7N7, and H5N1 are similar to each other but different from the host response to pdm09H1N1. On day 3, the responses to the avian viruses were similar to each other but different from the response to Mex4482 (Fig. 4A). Coagulation genes and LXR/RXR pathway genes were highly upregulated by Mex4482 but not by the avian viruses, suggesting that the avian viruses were potentially suppressing gene expression in these two pathways. There was also less induction of proinflammatory cytokine genes in mice infected with Mex4482 versus the others, suggesting that immune cell adhesion and trafficking were preferentially upregulated by the avian viruses (Fig. 4A). This was also reflected in our cellular infiltrate prediction using Gene Atlas v3; the lungs of Mex4482-infected mice were predicted to have lower levels of macrophages and granulocytes (Fig. 4C and D).

By day 5, the responses to all four viruses were overlapping. However, the ESs were higher for VN1203 versus the other viruses, indicating that VN1203 had a greater effect on these functional pathways by either up- or downregulating genes within each pathway. For example, the coagulation system had an ES of 15.5 in VN1203-infected mice, while it had ESs of 0.579, 5.94, and 1.54 in Mex4482-, NL219-, and Anhui1-infected mice, respectively. Mex4482-infected mice had the lowest ES for the cytokine-associated pathways associated with immune cell recruitment on day 5 (Fig. 4B), corroborating the resolution of the host response to Mex4482 that was suggested by the MDS plot and the DE gene analysis (Fig. 2).

We also performed hematoxylin and eosin (H&E) staining on lung tissue sections from mock-infected and virus-infected mice to validate the computational prediction of increased immune cell recruitment in the lungs of mice infected with the avian viruses. At 1, 3, and 5 days postinoculation, lungs from the mock-infected mice lacked lesions (Fig. 5A). Microscopic lesions were observed

Downloaded from http://jvi.asm.org/ on May 4, 2017 by COLUMBIA UNIVERSITY

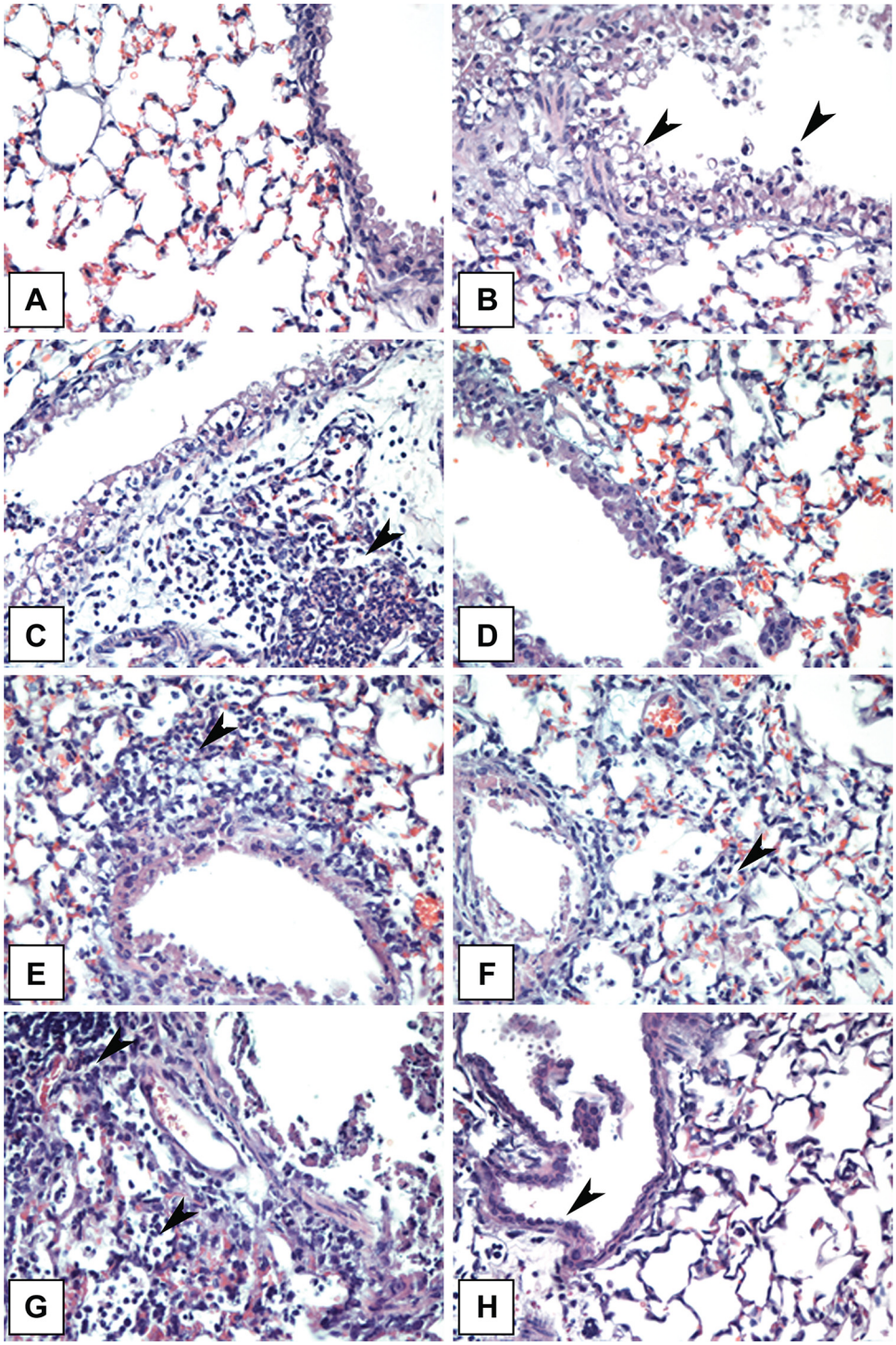

FIG 5 Histopathologic changes in tissues from influenza virus-infected mice. Photomicrographs of lung tissue sections stained with hematoxylin and eosin (magnification, ×400). (A) Lung tissue from mock-infected mouse on day 1 postinfection. (B) Vacuolation and necrosis of the respiratory epithelium (arrowheads) on day 1 in a mouse infected with H7N9 (A/Anhui/1/2013). (C) Moderate bronchiolitis with vacuolation and necrosis of the respiratory epithelium and associated peribronchiolar granulocytic inflammation (arrowhead) and edema on day 1 in a mouse infected with H5N1 (A/Vietnam/1203/2004). (D) Necrosis of respiratory epithelium with minimal alveolitis on day 3 in a mouse infected with pdm09H1N1 (A/Mexico/4482/2009). (E) Bronchiolitis with moderate peribronchial granulocytic alveolitis (arrowhead) on day 3 in a mouse infected with H5N1 (A/Vietnam/1203/2004). (F) Bronchiolitis and mild granulocytic alveolitis (arrowhead) on day 3 in a mouse infected with H7N7 (A/Netherlands/219/2003). (G) Necrosis of bronchial epithelium with associated granulocytic, histiocytic, and lymphocytic alveolitis (arrows) on day 3 in a mouse infected with H7N9 (A/Anhui/1/2013). (H) Regeneration of respiratory epithelium (arrowhead) on day 5 in a mouse infected with H1N1 (A/Mexico/4482/2007).

Downloaded from http://jvi.asm.org/ on May 4, 2017 by COLUMBIA UNIVERSITY

in H&E-stained lung tissue sections from infected mice. At day 1, mice in all four groups had minimal lesions, consisting of vacuolation and mild necrosis of the bronchial and bronchiolar epithelium (Fig. 5B), but two H5N1-infected mice also had mild to moderate peribronchial inflammation and mild accumulation of granulocytes in alveoli adjacent to bronchioles (Fig. 5C). On day 3, all four groups had focal to diffuse bronchiolar epithelial necrosis with associated peribronchiolar edema and mild to moderate inflammatory cell infiltrates (Fig. 5D, E, and F). However, the pdm09H1N1-infected mice had minimal alveolitis (Fig. 5D), while the H7N9-infected, H7N7-infected (Fig. 5E), and H5N1-infected (Fig. 5F) mice had mild to moderate alveolitis, with granulocytes being more common than mononuclear cells. On day 5, the H7N9-, H7N7-, and H5N1-infected mice had continuing necrosis of bronchiolar epithelium, peribronchiolar edema, and mild to moderate inflammation, with associated alveolitis (Fig. 5G). The lesions were moderately severe for H5N1- and H7N9-infected mice and continued to have significant granulocytic alveolitis adjacent to the airways, but macrophages predominated. The H7N7-infected mice had slightly less severe bronchiolitis and alveolitis, but macrophages were dominant among inflammatory cells. In contrast, the H1N1-infected mice had minimal lesions of mild peribronchiolar lymphocytic infiltrates and mild lymphocytic alveolitis without bronchiolar epithelial necrosis (Fig. 5H). Thus, histopathology data confirm the continuing necrotic and inflammatory processes in the lungs of H5N1-, H7N7-, and H7N9-infected mice, especially the prominence of macrophages in bronchioles and alveoli, but with some granulocytes, and the resolution of the cellular inflammatory processes with only minimal lesions in H1N1-infected mice.

Increased transcription of cytokine response genes and decreased transcription of coagulation and lipid metabolism genes correlate with increased pathogenicity. Despite the similarity of the NL219 and Anhui1 host responses to that of Mex4482 on day 1, infection with the H7 subtype viruses induced weight loss in mice, while infection with Mex4482 did not. Thus, we hypothesized that transcriptional changes that were common to Anhui1, NL219, and VN1203 but absent from Mex4482 would be contributors to disease and lethality. As some of the avian-virus-infected animals perished on day 5, we focused our analysis on days 1 and 3 to identify drivers of pathogenesis. As our group and others have shown previously, a robust cytokine response correlates with pathogenicity (21, 27, 37–39). We obtained similar results in this study, though the differences in the cytokine and interferon responses of the pathogenic viruses versus the nonpathogenic virus were not as prominent as in previous studies (Fig. 6A). The most striking difference between the host responses to the pathogenic versus the nonpathogenic viruses was that Mex4482-infected mice showed increased transcription of coagulation genes and lipid metabolism genes on day 3, while the avian virus-infected mice showed decreased transcription of these genes (Fig. 6B). Thus, viral pathogenicity correlated with lower expression of genes involved in lipid metabolism and coagulation. Importantly, this signature was not identified in the cell culture model (20), suggesting that it is driven by nonepithelial cell types or by the cross talk between multiple cell types in the lung.

Our data therefore suggest that the avian viruses induce a three-pronged transcriptomic signature of increased cytokine gene expression, decreased coagulation gene expression, and decreased lipid metabolism gene expression. This may be a general property of

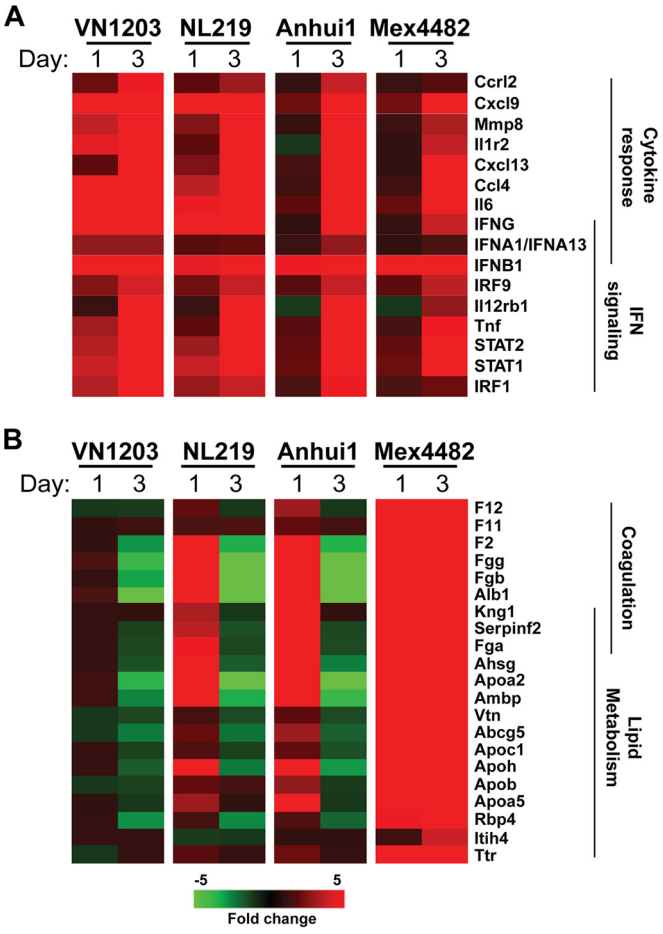

FIG 6 Pathogenic avian viruses induce a three-pronged signature of increased expression of cytokine response genes and decreased expression of coagulation and lipid metabolism genes. Heatmaps showing the expression levels of select cytokine and IFN signaling genes at days 1 and 3 postinfection (A) and the expression levels of selected coagulation and lipid metabolism genes at days 1 and 3 postinfection (B) from mice infected with H7N9 (A/Anhui/1/2013), H7N7 (A/Netherlands/219/2003), H5N1 (A/Vietnam/1203/2004), and pdm09H1N1 (A/Mexico/4482/2009).

pathogenic influenza viruses, as Josset et al. also showed that lethality of 1918 H1N1 and mouse-adapted pdm09H1N1 (A/California/04/2009) is associated with lower expression of lipid metabolism and coagulation genes (27). To determine the extent of the similarity between the transcriptional responses to the avian viruses and 1918 virus, we generated a heatmap using the gene list from Fig. 6B and expression values from the work of Josset et al. This analysis revealed the in-common suppression of coagulation and lipid metabolism genes (Fig. 7), suggesting that this signature is characteristic of pathogenic influenza viruses.

Prediction of potential antivirals against Anhui1 and other pathogenic influenza virus strains. Current treatments for influenza target the viral proteins, but this approach leads to the emergence of antiviral resistance because of the inherent malleability of the virus genome. Since dysregulated host pathways contribute to influenza pathogenesis, targeting the host response is a promising therapeutic approach (27, 37–42). We hypothesized that molecules that could reverse the common transcriptional response to the pathogenic viruses could be used to treat severe H7N9 influ-

Downloaded from http://jvi.asm.org/ on May 4, 2017 by COLUMBIA UNIVERSITY

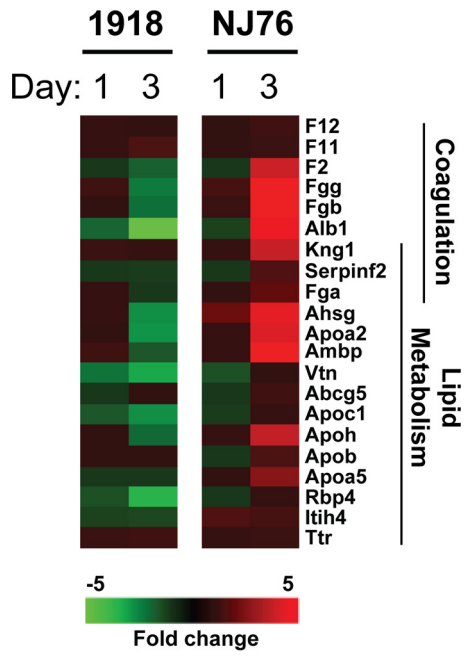

FIG 7 1918 H1N1 induces decreased expression of coagulation and lipid metabolism genes. Heatmaps show the expression levels of selected coagulation and lipid metabolism genes at days 1 and 3 postinfection from BALB/c mice infected with 10^6 PFU of pathogenic 1918 H1N1 or nonpathogenic A/New Jersey/8/76 (NJ76 H1N1). The experiment is described in reference 27, and the raw microarray data can be found at NCBI's Gene Expression Omnibus under GEO Series accession number GSE36328. Heatmaps were generated using the gene list from panel B and expression values from reference 27.

enza. To predict potential antivirals, we used IPA upstream regulator analysis to identify drugs and chemicals that could be used to treat infections caused by H7N9. The IPA database was queried with the DE genes from days 1 and 3 postinfection in Anhui1-infected mice, and we selected all the molecules annotated "drugs and chemicals" with Z scores less than −2. We identified 31 chemicals that were predicted to reverse transcriptional profiles associated with Anhui1 infection on days 1 and 3 postinfection; many of these were also predicted to reverse host responses to the other three viruses (Fig. 8). One of these molecules, minocycline, inhibits H7N9 replication *in vitro* (20). Six of these compounds, candesartan, dobutamine, warfarin, glyburide, minocycline, and eptifibatide, are FDA-approved drugs that could potentially be repurposed as treatments for H7N9 and other severe influenza virus infections.

DISCUSSION

After the Chinese government closed live-poultry markets in April 2013, the number of cases of H7N9 influenza diminished. However, there was a sharp increase in H7N9 cases during the 2013-2014 winter season. H7N9 has continued to circulate in the poultry population (9, 43, 44), raising the possibility of additional human infections. Since H7 subtype viruses have sporadically jumped to humans and caused severe disease (11), we need to understand their pathogenicity so as to identify novel interventions.

A striking result of our experiments was that all of the viruses examined replicated to similar levels but induced different tran-

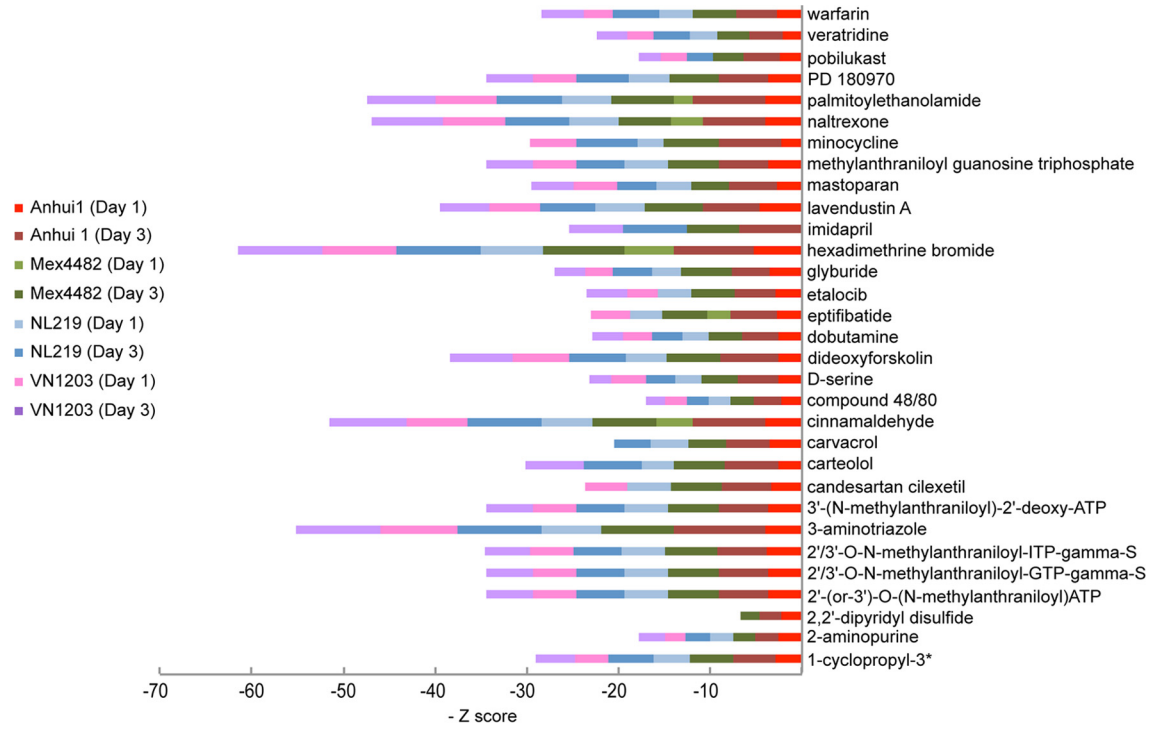

FIG 8 Molecules predicted to reverse the lung transcriptomic response to H7N9 and other influenza viruses. Drug prediction was based on the expression of known targets for molecules within the IPA database. For each virus, Z scores were calculated using log2FC expression of DE genes at days 1 and 3. A negative Z score indicates that the molecule downregulates genes that were significantly upregulated after infection and/or upregulates genes that were downregulated after infection. Thirty-one molecules were predicted to reverse the transcriptional profile associated with Anhui1 infection on days 1 and 3 postinfection. The Z scores associated with the other three viruses are also included for these 31 molecules. 1-Cyclopropyl-3*, 1-cyclopropyl-3-(3-(5-morpholin-4-ylmethyl-1H-benzoimidazol-2-yl)-1H-pyrazol-4-yl)urea.

Downloaded from http://jvi.asm.org/ on May 4, 2017 by COLUMBIA UNIVERSITY

scriptional responses in mice. Variation in morbidity and elicitation of proinflammatory cytokines and chemokines in murine lungs postinoculation among viruses which replicate to comparable titers has been demonstrated previously (14, 26, 35, 45), but a lack of in-depth transcriptomic analyses has limited our understanding of the responses that contribute to mammalian pathogenesis. Data in a recent paper attributed the higher cytokine production and pathogenicity induced by H5N1 versus H7N9 in mice to 10-fold-better replication of H5N1 virus in that model (33). This difference may be due in part to the virus strains used: we used A/Anhui/1/2013 (H7N9) and A/Vietnam/1203/2004 (H5N1), while Mok et al. used A/Shanghai/2/2013 (H7N9) and A/Hong Kong/483/97 (H5N1). Anhui1 elicits more weight loss in mice than Shanghai2 does and possesses a higher binding affinity than Shangai2 for all α2,3- and α2,6-glycans tested (15, 19). Subtle differences in receptor binding or other aspects of viral replication may impact infection kinetics, allowing Anhui1 to replicate to higher levels than Shangai2. Though virus load contributes to the host response (27, 33, 46), virus intrinsic properties are also important. Because all four viruses we examined replicated to comparable titers, we were able to ascribe differences in host response and pathogenicity to properties of the individual virus rather than to the quantity of virus present in the lungs. Our findings also illustrate a more general point: differences in the host response cannot be attributed solely to differences in viral replication.

Profiling of cultured airway cells had revealed that the epithelial transcriptomic response to Anhui1 was highly specific to this viral strain and that the Anhui1-induced response was more similar to the response to human H3N2 than to the responses to NL219 and VN1203 (20). Our current study revealed that additional differences and similarities in the responses arise among Anhui1, NL219, and VN1203 when the whole lung is profiled. VN1203, Anhui1, and NL219 were equally pathogenic in mice at a dose of 10^5 PFU, though there were differences in the quality and magnitude of the transcriptional responses that they elicited. When we compared the intensities of the host response using MDS and the number of DE genes, it was apparent that the host response to H5N1, particularly with respect to the interferon and cytokine responses, was more robust than the host response to the H7 subtype viruses. This is in accord with *in vitro* and *ex vivo* studies that have shown reduced induction of innate host responses among H7 subtype viruses compared with other virus subtypes in human respiratory and other cell types (20, 47–50). The lung host responses to H7N9 and H7N7 viruses were largely similar, but H7N7 induced a greater interferon and cytokine response than H7N9 on day 1. We also found that responses to the H7 subtype viruses share features with the responses to both VN1203 and Mex4482, which are strikingly different from each other. Our data therefore indicate that H7 subtype host responses are closer to the Mex4482 response than the VN1203 response early in infection but evolve to be similar to the VN1203 response as infection proceeds. Notably, though Anhui1 is a low-pathogenicity avian virus (LPAI) that does not cause disease in chickens, the murine response to it resembles the murine response to highly pathogenic NL219. This supports previous experiments showing that the basic sequence motif, which determines H7 subtype virulence in chickens, is not necessary for a virulent phenotype in mammals (23, 26).

Acute-phase serum samples from H7N9- and H5N1-infected patients contain elevated levels of inflammatory cytokines (9, 15, 51). Dysregulated cytokine responses are markers of influenza pathogenicity across multiple influenza virus serotypes (reviewed in reference 52). Our transcriptomic analysis corroborates previous studies showing that mice infected with H7N9, H5N1, and H7N7 also exhibit hypercytokinemia (13, 23, 33, 34, 36).

While the roles of lipid metabolism in influenza pathogenesis have been the subject of recent study, they are not well defined. ApoL2 inhibits apoptosis in human bronchial epithelial cells, while an ApoA1 mimetic inhibits the inflammatory response of pneumocytes (53, 54). Two recent papers also implicated lipid metabolism in influenza pathogenesis (40, 41), and protectin D1 (PD1), a fatty acid that inhibits monocyte and lymphocyte trafficking (55), was shown to decrease influenza virus replication and disease severity. Interleukin 1 (IL-1) receptor 1 knockout (IL-1R KO) mice show an increased susceptibility to influenza, and this correlates with decreased expression of lipid metabolism genes such as the ApoA2 and ApoH genes (56). Our group has previously shown that decreased expression of lipid metabolism genes is associated with the virulence of mouse-adapted pdm09H1N1 as well as 1918 H1N1 (27). Our current data extend the protective role of lipid metabolism to avian influenza viruses. Increased lipid metabolism may promote survival by increasing the cellular building blocks that are required for repairing damaged lung tissue and/or by producing anti-inflammatory lipids such as PD1 that diminish cytokine dysregulation and immune cell infiltration.

Coagulopathy has been observed in some cases of severe H7N9 and H5N1 influenza (3, 9, 57). Depressed coagulation factor transcription in the lungs of mice infected with pathogenic avian viruses may offer insight into these observations, especially since this has also been observed in mice infected with highly pathogenic H1N1 strains, such as the 1918 virus (27). Though the liver is the primary site of fibrinogen synthesis, lung epithelial cells also produce fibrinogen in response to inflammation, IL-6 treatment, and infection with severe acute respiratory syndrome coronavirus (SARS-CoV) or *Pneumocystis jirovecii* (58–61). H7N9 infection does not affect coagulation factor transcription in airway epithelial cells (20), suggesting that this signature is produced by other cells such as alveolar macrophages, which produce coagulation factors in response to stimulation (62). Coagulation factors may facilitate lung repair by increasing the conversion of fibrinogen into fibrin matrices, which act as scaffolds upon which damaged epithelium is repaired (63, 64). Additionally, increased coagulation factor expression could promote survival by decreasing infection-induced vascular permeability. The endothelial cells of the vasculature are considered central regulators of influenza-mediated cytokine dysregulation because increased vascular permeability leads to increased inflammatory cell recruitment (65). Activated protease-activated receptor 1 (PAR1) converts plasminogen (PLG) to plasmin, which increases vascular permeability through fibrinolysis, and PLG KO mice and PAR1 KO mice show increased survival when infected with H5N1, H3N2, or H1N1 influenza virus (66, 67). Pathogenic influenza virus infections could increase fibrinolysis, leading to vascular permeability, increased cellular infiltration, and irreparable lung damage. The increased expression of fibrinogen and other coagulation factors during nonpathogenic influenza virus infections may counteract fibrinolysis to decrease inflammation and promote survival. Fibrinogen treatment decreases bacterially induced lung pathogenesis (68), so it may be worth evaluating as a treatment for severe influenza.

Downloaded from http://jvi.asm.org/ on May 4, 2017 by COLUMBIA UNIVERSITY

We identified 31 drugs that were predicted to reverse the host response to Anhui1 in mice. Six of the predicted drugs are FDA approved, and of these six, dobutamine, candesartan, and minocycline have been shown to reduce lung damage in different experimental models. Dobutamine is a β-2 agonist that improves lung function in a rat lung model of hypothermia and ischemia (69), and it has been used to resolve acute lung damage in a human patient (70). Candesartan is an angiotensin receptor blocker that has been shown to reduce lung arteriolar hypertrophy in rats (71). Minocycline, a tetracycline antibiotic, is an attractive candidate because it inhibits Anhui1 replication in human airway cells (20) and decreases lung injury in mice (72).

In conclusion, our data suggest that severe influenza caused by avian viruses, such as H7N9, H7N7, and H5N1, or highly pathogenic human viruses, such as the 1918 virus, is associated with decreased transcription of lipid metabolism and coagulation genes and increased transcription of inflammatory cytokine genes. We have identified several FDA-approved compounds that may target this signature and which could be used to treat disease caused by H7N9 and other pathogenic influenza virus strains. Further study of the cross talk of cytokine signaling, coagulation response, and lipid metabolism in influenza pathogenesis will lead to a better understanding of severe influenza and could aid in the discovery of novel host-directed therapeutics for the treatment of severe influenza.

ACKNOWLEDGMENTS

This project was funded with federal funds from the NIH, NIAID Network of Centers of Excellence in Influenza Research and Surveillance (CEIRS), under contract HHSN266200700008C.

We thank John Treanor and David Topham at the University of Rochester for scientific discussions about the data and Marcus Korth and Adriana Forero for valuable feedback on the manuscript.

REFERENCES

1. **WHO.** 2014. WHO risk assessment: human infections with avian influenza A(H7N9) virus—21January 2014. WHO, Geneva, Switzerland. http://www.who.int/influenza/human_animal_interface/RiskAssessment_H7N9_21Jan14.pdf?ua=1.
2. **Claas EC, de Jong JC, van Beek R, Rimmelzwaan GF, Osterhaus AD.** 1998. Human influenza virus A/HongKong/156/97 (H5N1) infection. Vaccine **16:**977–978. http://dx.doi.org/10.1016/S0264-410X(98)00005-X.
3. **Claas EC, Osterhaus AD, van Beek R, De Jong JC, Rimmelzwaan GF, Senne DA, Krauss S, Shortridge KF, Webster RG.** 1998. Human influenza A H5N1 virus related to a highly pathogenic avian influenza virus. Lancet **351:**472–477. http://dx.doi.org/10.1016/S0140-6736(97)11212-0.
4. **CDC.** 2012. Notes from the field: highly pathogenic avian influenza A (H7N3) virus infection in poultry workers—Jalisco, Mexico, July 2012. MMWR Morb. Mortal. Wkly. Rep. **61:**726–727.
5. **Koopmans M, Wilbrink B, Conyn M, Natrop G, van der Nat Vennema HH, Meijer A, van Steenbergen J, Fouchier R, Osterhaus A, Bosman A.** 2004. Transmission of H7N7 avian influenza A virus to human beings during a large outbreak in commercial poultry farms in the Netherlands. Lancet **363:**587–593. http://dx.doi.org/10.1016/S0140-6736(04)15589-X.
6. **Puzelli S, Di Trani L, Fabiani C, Campitelli L, De Marco MA, Capua I, Aguilera JF, Zambon M, Donatelli I.** 2005. Serological analysis of serum samples from humans exposed to avian H7 influenza viruses in Italy between 1999 and 2003. J. Infect. Dis. **192:**1318–1322. http://dx.doi.org/10.1086/444390.
7. **ECDC.** 2014. Updated rapid risk assessment: human infection with a novel avian influenza A(H7N9) virus, China (third update)—27 January 2014. ECDC, Stockholm, Sweden. http://www.ecdc.europa.eu/en/publications/Publications/influenza-AH7N9-China-rapid-risk-assessment-27-January-2014.pdf.
8. **CDC.** 17 January 2014. Avian influenza A (H7N9) virus. CDC, Atlanta, GA. http://www.cdc.gov/flu/avianflu/h7n9-virus.htm.
9. **Chen Y, Liang W, Yang S, Wu N, Gao H, Sheng J, Yao H, Wo J, Fang Q, Cui D, Li Y, Yao X, Zhang Y, Wu H, Zheng S, Diao H, Xia S, Zhang Y, Chan KH, Tsoi HW, Teng JL, Song W, Wang P, Lau SY, Zheng M, Chan JF, To KK, Chen H, Li L, Yuen KY.** 2013. Human infections with the emerging avian influenza A H7N9 virus from wet market poultry: clinical analysis and characterisation of viral genome. Lancet **381:**1916–1925. http://dx.doi.org/10.1016/S0140-6736(13)60903-4.
10. **Gao R, Cao B, Hu Y, Feng Z, Wang D, Hu W, Chen J, Jie Z, Qiu H, Xu K, Xu X, Lu H, Zhu W, Gao Z, Xiang N, Shen Y, He Z, Gu Y, Zhang Z, Yang Y, Zhao X, Zhou L, Li X, Zou S, Zhang Y, Li X, Yang L, Guo J, Dong J, Li Q, Dong L, Zhu Y, Bai T, Wang S, Hao P, Yang W, Zhang Y, Han J, Yu H, Li D, Gao GF, Wu G, Wang Y, Yuan Z, Shu Y.** 2013. Human infection with a novel avian-origin influenza A (H7N9) virus. N. Engl. J. Med. **368:**1888–1897. http://dx.doi.org/10.1056/NEJMoa1304459.
11. **Morens DM, Taubenberger JK, Fauci AS.** 2013. H7N9 avian influenza A virus and the perpetual challenge of potential human pandemicity. mBio **4:**e00445–13. http://dx.doi.org/10.1128/mBio.00445-13.
12. **Richard M, Schrauwen EJ, de Graaf M, Bestebroer TM, Spronken MI, van Boheemen S, de Meulder D, Lexmond P, Linster M, Herfst S, Smith DJ, van den Brand JM, Burke DF, Kuiken T, Rimmelzwaan GF, Osterhaus AD, Fouchier RA.** 2013. Limited airborne transmission of H7N9 influenza A virus between ferrets. Nature **501:**560–563. http://dx.doi.org/10.1038/nature12476.
13. **Belser JA, Gustin KM, Pearce MB, Maines TR, Zeng H, Pappas C, Sun X, Carney PJ, Villanueva JM, Stevens J, Katz JM, Tumpey TM.** 2013. Pathogenesis and transmission of avian influenza A (H7N9) virus in ferrets and mice. Nature **501:**556–559. http://dx.doi.org/10.1038/nature12391.
14. **Watanabe T, Kiso M, Fukuyama S, Nakajima N, Imai M, Yamada S, Murakami S, Yamayoshi S, Iwatsuki-Horimoto K, Sakoda Y, Takashita E, McBride R, Noda T, Hatta M, Imai H, Zhao D, Kishida N, Shirakura M, de Vries RP, Shichinohe S, Okamatsu M, Tamura T, Tomita Y, Fujimoto N, Goto K, Katsura H, Kawakami E, Ishikawa I, Watanabe S, Ito M, Sakai-Tagawa Y, Sugita Y, Uraki R, Yamaji R, Eisfeld AJ, Zhong G, Fan S, Ping J, Maher EA, Hanson A, Uchida Y, Saito T, Ozawa M, Neumann G, Kida H, Odagiri T, Paulson JC, Hasegawa H, Tashiro M, Kawaoka Y.** 2013. Characterization of H7N9 influenza A viruses isolated from humans. Nature **501:**551–555. http://dx.doi.org/10.1038/nature12392.
15. **Zhou J, Wang D, Gao R, Zhao B, Song J, Qi X, Zhang Y, Shi Y, Yang L, Zhu W, Bai T, Qin K, Lan Y, Zou S, Guo J, Dong J, Dong L, Zhang Y, Wei H, Li X, Lu J, Liu L, Zhao X, Li X, Huang W, Wen L, Bo H, Xin L, Chen Y, Xu C, Pei Y, Yang Y, Zhang X, Wang S, Feng Z, Han J, Yang W, Gao GF, Wu G, Li D, Wang Y, Shu Y.** 2013. Biological features of novel avian influenza A (H7N9) virus. Nature **499:**500–503. http://dx.doi.org/10.1038/nature12379.
16. **Zhu H, Wang D, Kelvin DJ, Li L, Zheng Z, Yoon SW, Wong SS, Farooqui A, Wang J, Banner D, Chen R, Zheng R, Zhou J, Zhang Y, Hong W, Dong W, Cai Q, Roehrl MH, Huang SS, Kelvin AA, Yao T, Zhou B, Chen X, Leung GM, Poon LL, Webster RG, Webby RJ, Peiris JS, Guan Y, Shu Y.** 2013. Infectivity, transmission, and pathology of human-isolated H7N9 influenza virus in ferrets and pigs. Science **341:**183–186. http://dx.doi.org/10.1126/science.1239844.
17. **Tharakaraman K, Jayaraman A, Raman R, Viswanathan K, Stebbins NW, Johnson D, Shriver Z, Sasisekharan V, Sasisekharan R.** 2013. Glycan receptor binding of the influenza A virus H7N9 hemagglutinin. Cell **153:**1486–1493. http://dx.doi.org/10.1016/j.cell.2013.05.034.
18. **Shi Y, Zhang W, Wang F, Qi J, Wu Y, Song H, Gao F, Bi Y, Zhang Y, Fan Z, Qin C, Sun H, Liu J, Haywood J, Liu W, Gong W, Wang D, Shu Y, Wang Y, Yan J, Gao GF.** 2013. Structures and receptor binding of hemagglutinins from human-infecting H7N9 influenza viruses. Science **11:**243–247. http://dx.doi.org/10.1126/science.1242917.
19. **Zhang Q, Shi J, Deng G, Guo J, Zeng X, He X, Kong H, Gu C, Li X, Liu J, Wang G, Chen Y, Liu L, Liang L, Li Y, Fan J, Wang J, Li W, Guan L, Li Q, Yang H, Chen P, Jiang L, Guan Y, Xin X, Jiang Y, Tian G, Wang X, Qiao C, Li C, Bu Z, Chen H.** 2013. H7N9 influenza viruses are transmissible in ferrets by respiratory droplet. Science **341:**410–414. http://dx.doi.org/10.1126/science.1240532.
20. **Josset L, Zeng H, Kelly SM, Tumpey TM, Katze MG.** 2014. Transcriptomic characterization of the novel avian origin influenza A (H7N9) virus: specific and intermediate host-response between avian (H5N1 and H7N7) and human (H3N2) viruses and implications for treatment options. mBio **5:**e01102–13. http://dx.doi.org/10.1128/mBio.01102-13.

Downloaded from http://jvi.asm.org/ on May 4, 2017 by COLUMBIA UNIVERSITY

21. **Kash JC, Tumpey TM, Proll SC, Carter V, Perwitasari O, Thomas MJ, Basler CF, Palese P, Taubenberger JK, Garcia-Sastre A, Swayne DE, Katze MG.** 2006. Genomic analysis of increased host immune and cell death responses induced by 1918 influenza virus. Nature **443:**578–581. http://dx.doi.org/10.1038/nature05181.
22. **Cilloniz C, Pantin-Jackwood MJ, Ni C, Goodman AG, Peng X, Proll SC, Carter VS, Rosenzweig ER, Szretter KJ, Katz JM, Korth MJ, Swayne DE, Tumpey TM, Katze MG.** 2010. Lethal dissemination of H5N1 influenza virus is associated with dysregulation of inflammation and lipoxin signaling in a mouse model of infection. J. Virol. **84:**7613–7624. http://dx.doi.org/10.1128/JVI.00553-10.
23. **Belser JA, Lu X, Maines TR, Smith C, Li Y, Donis RO, Katz JM, Tumpey TM.** 2007. Pathogenesis of avian influenza (H7) virus infection in mice and ferrets: enhanced virulence of Eurasian H7N7 viruses isolated from humans. J. Virol. **81:**11139–11147. http://dx.doi.org/10.1128/JVI.01235-07.
24. **Fouchier RA, Schneeberger PM, Rozendaal FW, Broekman JM, Kemink SA, Munster V, Kuiken T, Rimmelzwaan GF, Schutten M, Van Doornum GJ, Koch G, Bosman A, Koopmans M, Osterhaus AD.** 2004. Avian influenza A virus (H7N7) associated with human conjunctivitis and a fatal case of acute respiratory distress syndrome. Proc. Natl. Acad. Sci. U. S. A. **101:**1356–1361. http://dx.doi.org/10.1073/pnas.0308352100.
25. **de Wit E, Munster VJ, Spronken MI, Bestebroer TM, Baas C, Beyer WE, Rimmelzwaan GF, Osterhaus AD, Fouchier RA.** 2005. Protection of mice against lethal infection with highly pathogenic H7N7 influenza A virus by using a recombinant low-pathogenicity vaccine strain. J. Virol. **79:**12401–12407. http://dx.doi.org/10.1128/JVI.79.19.12401-12407.2005.
26. **Joseph T, McAuliffe J, Lu B, Jin H, Kemble G, Subbarao K.** 2007. Evaluation of replication and pathogenicity of avian influenza A H7 subtype viruses in a mouse model. J. Virol. **81:**10558–10566. http://dx.doi.org/10.1128/JVI.00970-07.
27. **Josset L, Belser JA, Pantin-Jackwood MJ, Chang JH, Chang ST, Belisle SE, Tumpey TM, Katze MG.** 2012. Implication of inflammatory macrophages, nuclear receptors, and interferon regulatory factors in increased virulence of pandemic 2009 H1N1 influenza A virus after host adaptation. J. Virol. **86:**7192–7206. http://dx.doi.org/10.1128/JVI.00563-12.
28. **Zeng H, Goldsmith C, Thawatsupha P, Chittaganpitch M, Waicharoen S, Zaki S, Tumpey TM, Katz JM.** 2007. Highly pathogenic avian influenza H5N1 viruses elicit an attenuated type i interferon response in polarized human bronchial epithelial cells. J. Virol. **81:**12439–12449. http://dx.doi.org/10.1128/JVI.01134-07.
29. **Smyth GK.** 2005. Limma: linear models for microarray data, p 397–420. *In* Gentleman R, Carey VJ, Huber W, Irizarry RA, Dudoit S (ed), Bioinformatics and computational biology solutions using R and Bioconductor. Springer, New York, NY.
30. **Kruskal JB, Wish M.** 1978. Multidimensional scaling. Methods **116:**463–504.
31. **Venables WN, Ripley BD.** 2002. Modern applied statistics with S (statistics and computing). Springer, New York, NY.
32. **Baranovich T, Burnham AJ, Marathe BM, Armstrong J, Guan Y, Shu Y, Peiris JM, Webby RJ, Webster RG, Govorkova EA.** 2013. The neuraminidase inhibitor oseltamivir is effective against A/Anhui/1/2013 (H7N9) influenza virus in a mouse model of acute respiratory distress syndrome. J. Infect. Dis. http://dx.doi.org/10.1093/infdis/jit554.
33. **Mok CK, Lee HH, Chan MC, Sia SF, Lestra M, Nicholls JM, Zhu H, Guan Y, Peiris JM.** 2013. Pathogenicity of the novel A/H7N9 influenza virus in mice. mBio **4:**e00362–13. http://dx.doi.org/10.1128/mBio.00362-13.
34. **Gao P, Watanabe S, Ito T, Goto H, Wells K, McGregor M, Cooley AJ, Kawaoka Y.** 1999. Biological heterogeneity, including systemic replication in mice, of H5N1 influenza A virus isolates from humans in Hong Kong. J. Virol. **73:**3184–3189.
35. **Lu X, Tumpey TM, Morken T, Zaki SR, Cox NJ, Katz JM.** 1999. A mouse model for the evaluation of pathogenesis and immunity to influenza A (H5N1) viruses isolated from humans. J. Virol. **73:**5903–5911.
36. **Maines TR, Lu XH, Erb SM, Edwards L, Guarner J, Greer PW, Nguyen DC, Szretter KJ, Chen LM, Thawatsupha P, Chittaganpitch M, Waicharoen S, Nguyen DT, Nguyen T, Nguyen HH, Kim JH, Hoang LT, Kang C, Phuong LS, Lim W, Zaki S, Donis RO, Cox NJ, Katz JM, Tumpey TM.** 2005. Avian influenza (H5N1) viruses isolated from humans in Asia in 2004 exhibit increased virulence in mammals. J. Virol. **79:**11788–11800. http://dx.doi.org/10.1128/JVI.79.18.11788-11800.2005.
37. **Brandes M, Klauschen F, Kuchen S, Germain RN.** 2013. A systems analysis identifies a feedforward inflammatory circuit leading to lethal influenza infection. Cell **154:**197–212. http://dx.doi.org/10.1016/j.cell.2013.06.013.
38. **Chang ST, Tchitchek N, Ghosh D, Benecke A, Katze MG.** 2011. A chemokine gene expression signature derived from meta-analysis predicts the pathogenicity of viral respiratory infections. BMC Syst. Biol. **5:**202. http://dx.doi.org/10.1186/1752-0509-5-202.
39. **Tchitchek N, Eisfeld AJ, Tisoncik-Go J, Josset L, Gralinski LE, Becavin C, Tilton SC, Webb-Robertson BJ, Ferris MT, Totura AL, Li C, Neumann G, Metz TO, Smith RD, Waters KM, Baric R, Kawaoka Y, Katze MG.** 2013. Specific mutations in H5N1 mainly impact the magnitude and velocity of the host response in mice. BMC Syst. Biol. **7:**69. http://dx.doi.org/10.1186/1752-0509-7-69.
40. **Morita M, Kuba K, Ichikawa A, Nakayama M, Katahira J, Iwamoto R, Watanebe T, Sakabe S, Daidoji T, Nakamura S, Kadowaki A, Ohto T, Nakanishi H, Taguchi R, Nakaya T, Murakami M, Yoneda Y, Arai H, Kawaoka Y, Penninger JM, Arita M, Imai Y.** 2013. The lipid mediator protectin D1 inhibits influenza virus replication and improves severe influenza. Cell **153:**112–125. http://dx.doi.org/10.1016/j.cell.2013.02.027.
41. **Tam VC, Quehenberger O, Oshansky CM, Suen R, Armando AM, Treuting PM, Thomas PG, Dennis EA, Aderem A.** 2013. Lipidomic profiling of influenza infection identifies mediators that induce and resolve inflammation. Cell **154:**213–227. http://dx.doi.org/10.1016/j.cell.2013.05.052.
42. **Watanabe T, Tisoncik-Go J, Tchitchek N, Watanabe S, Benecke AG, Katze MG, Kawaoka Y.** 2013. 1918 Influenza virus hemagglutinin (HA) and the viral RNA polymerase complex enhance viral pathogenicity, but only HA induces aberrant host responses in mice. J. Virol. **87:**5239–5254. http://dx.doi.org/10.1128/JVI.02753-12.
43. **Lam TT, Wang J, Shen Y, Zhou B, Duan L, Cheung CL, Ma C, Lycett SJ, Leung CY, Chen X, Li L, Hong W, Chai Y, Zhou L, Liang H, Ou Z, Liu Y, Farooqui A, Kelvin DJ, Poon LL, Smith DK, Pybus OG, Leung GM, Shu Y, Webster RG, Webby RJ, Peiris JS, Rambaut A, Zhu H, Guan Y.** 2013. The genesis and source of the H7N9 influenza viruses causing human infections in China. Nature http://dx.doi.org/10.1038/nature12515.
44. **Wang C, Wang J, Su W, Gao S, Luo J, Zhang M, Xie L, Liu S, Liu X, Chen Y, Jia Y, Zhang H, Ding H, He H.** 2014. Relationship between domestic and wild birds in live poultry market and a novel human H7N9 virus in China. J. Infect. Dis. **209:**34–37. http://dx.doi.org/10.1093/infdis/jit478.
45. **Belser JA, Wadford DA, Pappas C, Gustin KM, Maines TR, Pearce MB, Zeng H, Swayne DE, Pantin-Jackwood M, Katz JM, Tumpey TM.** 2010. Pathogenesis of pandemic influenza A (H1N1) and triple-reassortant swine influenza A (H1) viruses in mice. J. Virol. **84:**4194–4203. http://dx.doi.org/10.1128/JVI.02742-09.
46. **Boon AC, Finkelstein D, Zheng M, Liao G, Allard J, Klumpp K, Webster R, Peltz G, Webby RJ.** 2011. H5N1 influenza virus pathogenesis in genetically diverse mice is mediated at the level of viral load. mBio **2:**e00171–11. http://dx.doi.org/10.1128/mBio.00171-11.
47. **Belser JA, Zeng H, Katz JM, Tumpey TM.** 2011. Infection with highly pathogenic H7 influenza viruses results in an attenuated proinflammatory cytokine and chemokine response early after infection. J. Infect. Dis. **203:**40–48. http://dx.doi.org/10.1093/infdis/jiq018.
48. **Belser JA, Gustin KM, Maines TR, Blau DM, Zaki SR, Katz JM, Tumpey TM.** 2011. Pathogenesis and transmission of triple-reassortant swine H1N1 influenza viruses isolated before the 2009 H1N1 pandemic. J. Virol. **85:**1563–1572. http://dx.doi.org/10.1128/JVI.02231-10.
49. **Chan MCW, Chan RWY, Chan LLY, Mok CKP, Hui KPY, Fong JHM, Tao KP, Poon LLM, Nicholls JM, Guan Y, Peiris JM.** 2013. Tropism and innate host responses of a novel avian influenza A H7N9 virus: an analysis of ex-vivo and in-vitro cultures of the human respiratory tract. Lancet Respir. Med. **1:**534–542. http://dx.doi.org/10.1016/S2213-2600(13)70138-3.
50. **Friesenhagen J, Boergeling Y, Hrincius E, Ludwig S, Roth J, Viemann D.** 2012. Highly pathogenic avian influenza viruses inhibit effective immune responses of human blood-derived macrophages. J. Leukoc. Biol. **92:**11–20. http://dx.doi.org/10.1189/jlb.0911479.
51. **de Jong MD, Simmons CP, Thanh TT, Hien VM, Smith GJ, Chau TN, Hoang DM, Chau NV, Khanh TH, Dong VC, Qui PT, Cam BV, Ha do, Guan QY, Peiris JS, Chinh NT, Hien TT, Farrar J.** 2006. Fatal outcome of human influenza A (H5N1) is associated with high viral load and hypercytokinemia. Nat. Med. **12:**1203–1207. http://dx.doi.org/10.1038/nm1477.

Downloaded from http://jvi.asm.org/ on May 4, 2017 by COLUMBIA UNIVERSITY

52. **Tisoncik JR, Korth MJ, Simmons CP, Farrar J, Martin TR, Katze MG.** 2012. Into the eye of the cytokine storm. Microbiol. Mol. Biol. Rev. **76:**16–32. http://dx.doi.org/10.1128/MMBR.05015-11.
53. **Liao W, Goh FY, Betts RJ, Kemeny DM, Tam J, Bay BH, Wong WS.** 2011. A novel anti-apoptotic role for apolipoprotein L2 in IFN-gamma-induced cytotoxicity in human bronchial epithelial cells. J. Cell. Physiol. **226:**397–406. http://dx.doi.org/10.1002/jcp.22345.
54. **Van Lenten BJ, Wagner AC, Navab M, Anantharamaiah GM, Hui EK, Nayak DP, Fogelman AM.** 2004. D-4F, an apolipoprotein A-I mimetic peptide, inhibits the inflammatory response induced by influenza A infection of human type II pneumocytes. Circulation **110:**3252–3258. http://dx.doi.org/10.1161/01.CIR.0000147232.75456.B3.
55. **Serhan CN, Gotlinger K, Hong S, Lu Y, Siegelman J, Baer T, Yang R, Colgan SP, Petasis NA.** 2006. Anti-inflammatory actions of neuroprotectin D1/protectin D1 and its natural stereoisomers: assignments of dihydroxy-containing docosatrienes. J. Immunol. **176:**1848–1859. http://dx.doi.org/10.4049/jimmunol.176.3.1848.
56. **Belisle SE, Tisoncik JR, Korth MJ, Carter VS, Proll SC, Swayne DE, Pantin-Jackwood M, Tumpey TM, Katze MG.** 2010. Genomic profiling of tumor necrosis factor alpha (TNF-alpha) receptor and interleukin-1 receptor knockout mice reveals a link between TNF-alpha signaling and increased severity of 1918 pandemic influenza virus infection. J. Virol. **84:**12576–12588. http://dx.doi.org/10.1128/JVI.01310-10.
57. **Chen E, Wang F, Lv H, Zhang Y, Ding H, Liu S, Cai J, Xie L, Xu X, Chai C, Mao H, Sun J, Lin J, Yu Z, Li L, Chen Z, Xia S.** 2013. The first avian influenza A (H7N9) viral infection in humans in Zhejiang Province, China: a death report. Front. Med. **7:**333–344. http://dx.doi.org/10.1007/s11684-013-0275-1.
58. **Haidaris PJ.** 1997. Induction of fibrinogen biosynthesis and secretion from cultured pulmonary epithelial cells. Blood **89:**873–882.
59. **Duan HO, Simpson-Haidaris PJ.** 2006. Cell type-specific differential induction of the human gamma-fibrinogen promoter by interleukin-6. J. Biol. Chem. **281:**12451–12457. http://dx.doi.org/10.1074/jbc.M600294200.
60. **Tan YJ, Tham PY, Chan DZ, Chou CF, Shen S, Fielding BC, Tan TH, Lim SG, Hong W.** 2005. The severe acute respiratory syndrome coronavirus 3a protein up-regulates expression of fibrinogen in lung epithelial cells. J. Virol. **79:**10083–10087. http://dx.doi.org/10.1128/JVI.79.15.10083-10087.2005.
61. **Simpson-Haidaris PJ, Courtney MA, Wright TW, Goss R, Harmsen A, Gigliotti F.** 1998. Induction of fibrinogen expression in the lung epithelium during Pneumocystis carinii pneumonia. Infect. Immun. **66:**4431–4439.
62. **Chapman HA, Jr, Allen CL, Stone OL, Fair DS.** 1985. Human alveolar macrophages synthesize factor VII in vitro. Possible role in interstitial lung disease. J. Clin. Invest. **75:**2030–2037.
63. **Van Leer C, Stutz M, Haeberli A, Geiser T.** 2005. Urokinase plasminogen activator released by alveolar epithelial cells modulates alveolar epithelial repair in vitro. Thromb. Haemost. **94:**1257–1264.
64. **Perrio MJ, Ewen D, Trevethick MA, Salmon GP, Shute JK.** 2007. Fibrin formation by wounded bronchial epithelial cell layers in vitro is essential for normal epithelial repair and independent of plasma proteins. Clin. Exp. Allergy **37:**1688–1700. http://dx.doi.org/10.1111/j.1365-2222.2007.02829.x.
65. **Teijaro JR, Walsh KB, Cahalan S, Fremgen DM, Roberts E, Scott F, Martinborough E, Peach R, Oldstone MB, Rosen H.** 2011. Endothelial cells are central orchestrators of cytokine amplification during influenza virus infection. Cell **146:**980–991. http://dx.doi.org/10.1016/j.cell.2011.08.015.
66. **Khoufache K, Berri F, Nacken W, Vogel AB, Delenne M, Camerer E, Coughlin SR, Carmeliet P, Lina B, Rimmelzwaan GF, Planz O, Ludwig S, Riteau B.** 2013. PAR1 contributes to influenza A virus pathogenicity in mice. J. Clin. Invest. **123:**206–214. http://dx.doi.org/10.1172/JCI61667.
67. **Berri F, Rimmelzwaan GF, Hanss M, Albina E, Foucault-Grunenwald ML, Le VB, Vogelzang-van Trierum SE, Gil P, Camerer E, Martinez D, Lina B, Lijnen R, Carmeliet P, Riteau B.** 2013. Plasminogen controls inflammation and pathogenesis of influenza virus infections via fibrinolysis. PLoS Pathog. **9:**e1003229. http://dx.doi.org/10.1371/journal.ppat.1003229.
68. **Yang H, Ko HJ, Yang JY, Kim JJ, Seo SU, Park SG, Choi SS, Seong JK, Kweon MN.** 2013. Interleukin-1 promotes coagulation, which is necessary for protective immunity in the lung against Streptococcus pneumoniae infection. J. Infect. Dis. **207:**50–60. http://dx.doi.org/10.1093/infdis/jis651.
69. **Dacho C, Dacho A, Geissler A, Hauser C, Nowak K, Beck G.** 2013. Catecholamines reduce dose-dependent oedema formation and inflammatory reaction in an isolated rat lung model. In Vivo **27:**49–56.
70. **de Chazal I, Parham WM, III, Liopyris P, Wijdicks EF.** 2005. Delayed cardiogenic shock and acute lung injury after aneurysmal subarachnoid hemorrhage. Anesth. Analg. **100:**1147–1149. http://dx.doi.org/10.1213/01.ANE.0000147704.90285.2A.
71. **Kishi K, Jin D, Takai S, Muramatsu M, Katayama H, Tamai H, Miyazaki M.** 2006. Role of chymase-dependent angiotensin II formation in monocrotaline-induced pulmonary hypertensive rats. Pediatr. Res. **60:**77–82. http://dx.doi.org/10.1203/01.pdr.0000219431.45075.d9.
72. **Kalemci S, Dirican N, Cetin ES, Sozen H, Uner AG, Yaylali A, Aksun S, Karacam V, Ulger E, Sutcu R, Dirican A.** 2013. The efficacy of minocycline against methotrexate-induced pulmonary fibrosis in mice. Eur. Rev. Med. Pharmacol. Sci. **17:**3334–3340.

Downloaded from http://jvi.asm.org/ on May 4, 2017 by COLUMBIA UNIVERSITY